Chemical Vapor Deposition

DOI: 10.1002/cvde.200606576

Full Paper

Incubation Effects upon Polycrystalline Silicon on Glass Deposited by Hot-Wire CVD**

By *Shui-Yang Lien*, *Hsin-Yuan Mao*, *Bing-Rui Wu*, *Ray-Hua Horng*, and *Dong-Sing Wuu**

A growth mechanism diagnosis for high-rate, polycrystalline silicon deposition using hot-wire CVD is explored in this article. The effects of various deposition parameters on the Si film growth are investigated by Raman spectroscopy and transmission electron microscopy (TEM) measurements, with special attention paid to the crystalline and amorphous phases. It is found that the H_2/SiH_4 ratio and substrate temperature (T_s) are the essential process parameters in determining the crystalline phase and the incubation thickness of the as-deposited Si film. Under low hydrogen dilution conditions, an amorphous incubation layer was formed and degraded the crystalline fraction of the Si film. The incubation thickness prior to the nucleation decreases with the increase of the hydrogen dilution ratio. Under higher H_2/SiH_4 ratios (≥50), the amorphous phase deposited on the substrate could be etched selectively by the atomic hydrogen. As a consequence, nucleation of small crystallite occurs directly on the substrate. At low substrate temperatures, the deposition process shows the disadvantages of small grain size and low crystallinity. The poly-Si film can be deposited from the seed layer under high T_s conditions (>350 °C) where the Si appears singly crystallized at the initial stage and then grows epitaxially.

Keywords: Growth mechanism, Hot-wire CVD, Polycrystalline silicon, Raman spectroscopy, Transmission electron microscopy

1. Introduction

Recently, polycrystalline silicon (poly-Si) and microcrystalline silicon (μc-Si) thin films prepared at low temperatures have attracted significant attention because of their potential application for low-cost, large-area solar cells. As compared with the bulk-type solar cell, Si thin-film solar cells are expected to achieve lower production cost due to the lower thermal budget and smaller amount of silicon material used. The plasma-enhanced (PE) CVD technique has been developed and studied for many years. Up to now, the low deposition rate is considered a bottleneck for the industrial production of Si thin-film solar cells. This is indeed important, while at high rate it is also becoming increasingly difficult to maintain a constant crystalline fraction over the entire thickness of the layer due to the development of amorphous and crystalline volume fraction at different rates. Hot-wire (HW) CVD,[1] also called catalytic (C) CVD,[2] is a promising technology for obtaining device-quality poly-Si material at high deposition rates.[3,4] The n-i-p cells using poly-Si as the i-layer have been investigated by many groups, yielding efficiencies greater than 7 %.[5–8]

Hydrogenated amorphous silicon (a-Si:H) films can be obtained using HWCVD with pure silane without hydrogen dilution. This has received considerable attention as an alternative approach for the synthesis of a-Si:H.[1,2] In the HWCVD process, the hydrogen/silane gas mixture ratio (H_2/SiH_4) and substrate temperature (T_s) were confirmed to have large effects on the microstructure of the Si film, such as Si phase transition from amorphous to microcrystalline and polycrystalline.[9,10] It is well known that μc-Si or poly-Si deposition is an inhomogeneous growth process. The deposition generally begins with an amorphous phase. It needs a minimum thickness, called the incubation phase, before a localized phase transformation, called nucleation, takes place. Although the exact nucleation mechanism is still not understood, models for the phase transformation and nucleation process have been proposed.[11–16] To obtain more insight into the growth mechanism of poly-Si deposited by HWCVD on the glass substrate, Raman spectroscopy and high resolution (HR) TEM studies have been performed on layers deposited using various H_2/SiH_4 ratios and substrate temperatures.

[*] Prof. D. S. Wuu, S. Y. Lien, H. Y. Mao, B. R. Wu
Department of Materials Science and Engineering, National Chung Hsing University
Taichung, Taiwan 40227 (Taiwan R.O.C.)
E-mail: dsw@dragon.nchu.edu.tw
Prof. R. H. Horng
Institute of Precision Engineering, National Chung Hsing University
Taichung, Taiwan 40227 (Taiwan R.O.C.)

[**] This work was supported by the National Science Council of the Republic of China under contract No. NSC 093-ET-7-005-001-ET.

2. Results and Discussion

The as-deposited Si thin films were analyzed using the Raman scattering spectroscopy to reveal their crystalline structure more quantitatively. Typically, the spectrum could be resolved into several components in the region from 400 to 550 cm^{-1}, assuming Gaussian line shapes. The Raman signal due to the transverse optical mode was deconvoluted into three components: I_c (approx. 520 cm^{-1}, crystalline phase with a grain size larger than 10 nm), I_m (approx. 510 cm^{-1}, crystalline phase with a grain size smaller than 10 nm), and I_a (approx. 480 cm^{-1}, amorphous phase).[17] The crystalline fraction (X_c) was defined as $X_c = (I_c + I_m)/(I_c + I_m + I_a)$. This approach has been successful in explaining the spectral structure of Raman scattering from small silicon particles.[18] When the crystalline mode was higher than the amorphous-like one, it separated into two parts; one with a peak at about 520 cm^{-1}, and the other appearing as a broader mode at about 510 cm^{-1}. The separation could probably be caused by the distribution of crystallite size (as mentioned above). In our studies, the Raman spectra reveal a doping level of the grown layers since the spectra intensity between 400 and 450 cm^{-1} is higher than the intensity above 550 cm^{-1}. To examine any possible metallic contamination in these HWCVD Si films, secondary ion mass spectroscopy (SIMS) measurements were performed on these samples. It was found that only oxygen and carbon impurity atoms in the Si film can be detected, and their concentrations were determined to be 2×10^{15} and 6×10^{15} cm^{-3}, respectively. The metal impurities in the as-deposited Si films are below our SIMS detection limit. Similar Raman spectra (regarding the intensities of ~400–450, and above 550 cm^{-1}) have also been reported by other workers.[19–21]

The effect of the H_2/SiH_4 ratio on the Raman spectra of the Si thin films is shown in Figure 1. Here the substrate temperature (T_s) was maintained at 350 °C because a clear phase transformation of the Si crystallinity can be observed over these H_2/SiH_4 ratios. Apart from this temperature, the crystalline phase change of the Si film is not obvious in our experimental range. For the sample deposited using a low hydrogen dilution ratio (e.g., $H_2/SiH_4 = 5$), the spectrum exhibits a typical microcrystal feature where a peak centered at 513 cm^{-1} with a full width at half maximum (FWHM) of 27.5 cm^{-1}. The crystalline Si is calibrated at 520 cm^{-1}. When the H_2/SiH_4 ratio increases to 25, the Raman peak shifts to 519 cm^{-1} which indicates poly-Si growth. That is, the deposition condition is within the transition region from the amorphous to polycrystalline phase. This could be due to the thickness of the amorphous incubation layer decreasing and the film tending to become thinner as the H_2 dilution ratio increases. Under higher H_2/SiH_4 ratios (≥50), the amorphous phase deposited on the substrate could be etched selectively by the atomic hydrogen. In consequence, nucleation of small crystallites occurs directly on the substrate.[22] The corresponding X_c and FWHM as functions of

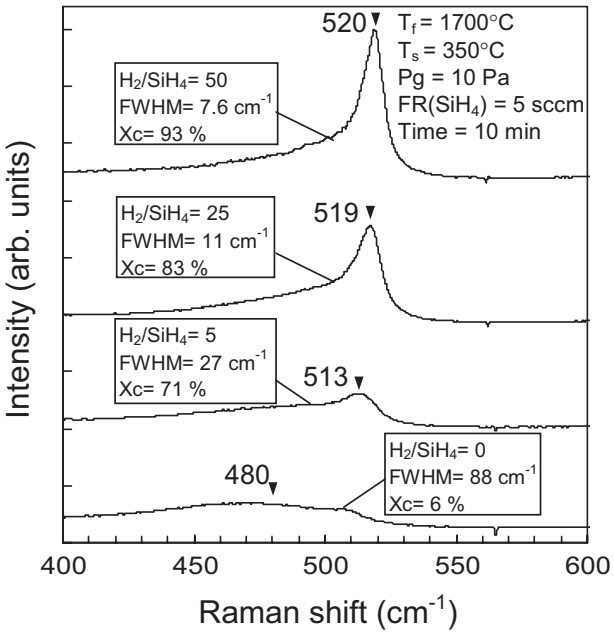

Fig. 1. Raman spectra of silicon films deposited by HWCVD at various hydrogen dilution ratios, the volume fraction of crystalline silicon X_c, and FWHM of silicon films as a function of hydrogen dilution ratio.

the hydrogen dilution ratio are also shown in Figure 1. For the sample deposited using $H_2/SiH_4 = 50$, X_c can increase to 93 % with an FWHM of 7.6 cm^{-1}.

There are two hydrogen dilution ratio regimes. In the high hydrogen dilution process, the ratio is 50, whereas in the low hydrogen dilution process, the ratio is 5. The substrate temperature was kept at 350 °C. Poly-Si films are grown at high hydrogen dilution. We observed that the nucleation process and the structure sensitively depend on the hydrogen dilution ratio. Figure 2 shows the TEM results of poly-Si films deposited at a hydrogen dilution ratio of 50. The crystalline structure of this sample has determined to be $X_c = 93$ % from the Raman analysis. The dark field (DF) image of a fully crystallized sample is presented in Figure 2a. Although the individual crystallites are quite large, they are very irregular in shape. The diffraction patterns (inset above) show the polycrystalline structure of the sample. Halo patterns corresponding to amorphous silicon are not observed, indicating that the layer is completely crystallized. The measured radii of diffraction arc rings correspond to (220) and (311) preferential orientation. The textured ring patterns where the rings are more intense is over a certain angular range. A DF image (Fig. 2a) of the textured grains shows an equiaxed structure. The specimen is textured about a direction at an angle to the beam, so the Ewald sphere creates elongated spots or arcs in the diffraction pattern. Figure 2a (inset below) also shows the convergent-beam electron diffraction (CBED) pattern from film on a grain. CBED can be used to analyze areas ~100 nm in diameter. Clear diffraction spots indicating a highly ordered structure are seen, implying that each grain

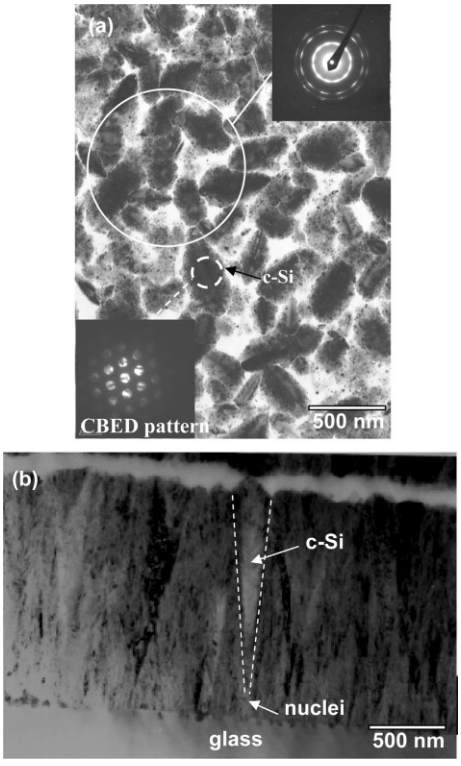

Fig. 2. TEM images of HWCVD poly-Si film; (a) dark field image and diffraction pattern, (b) cross-section image. The sample was fabricated under an SiH_4 flow rate of 5 sccm, a H_2 flow rate of 250 sccm, a filament temperature of 1700 °C, and a substrate temperature of 350 °C.

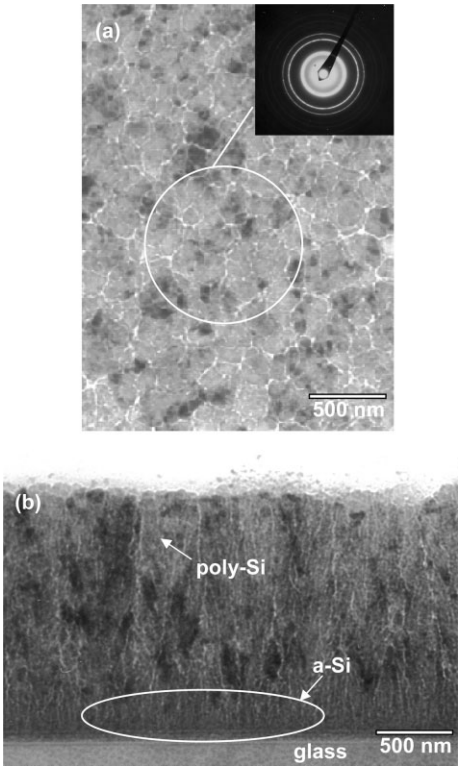

Fig. 3. TEM imags of HWCVD μc-Si film; (a) dark field image and diffraction pattern, (b) cross-section image. The sample was fabricated under an SiH_4 flow rate of 5 sccm, a H_2 flow rate of 25 sccm, a filament temperature of 1700 °C, and a substrate temperature of 350 °C.

in this region consists of crystalline phases of mainly single domain. Figure 2b shows the cross-section TEM image of poly-Si film deposited at high hydrogen dilution. Nucleation starts immediately at the interface. The films tend to process better initial crystalline growth from the glass substrate. This can eliminate the amorphous incubation layer and fabricate device-quality poly-Si films avoiding any amorphous incubation phase. The observed high crystalline structures agree well with the Raman results.

The dilution of silane precursor in hydrogen to favor the polysilicon growth is already known in the microelectronics field. However, due to the difference in growth mechanism, Si thin films with high hydrogen content (~10 %) can be obtained in typical PECVD systems. For the HWCVD process, Si thin films with low hydrogen content (~1 %) are easily obtained. This is due to that fact that a large amount of H atoms formed H_2 and leave during the process of Si deposition. Several researchers have previously compared the properties of Si films prepared by HWCVD and PECVD.[23–25] However, there are few reports about the crystalline evolution of the HWCVD Si films. In order to give a more comprehensive view, the growth mechanism of HWCVD poly-Si films was probed and interpreted by both the Raman and TEM examinations.

TEM images of the Si film deposited at low hydrogen dilution ($H_2/SiH_4 = 5$) are shown in Figure 3. The crystalline structure of this sample has determined from the Raman analysis to be $X_c = 73$ %. It is observed that there is an incubation phase of the amorphous Si growth. In general, an amorphous phase is preferentially fabricated on the glass substrate in the initial stage. Some of the nuclei predominate over the others and the columnar crystals start to grow on the nuclei with a compact structure. That is, the growth is not homogeneous in that the V shaped columns start at different depths. The grain boundaries are mixed and not sharp. Under low hydrogen dilution conditions, an amorphous incubation layer was formed and affected the subsequent silicon growth. This would degrade the crystalline fraction of the Si film, which agreed well with the Raman result as described in Figure 1. Based on the results from Figures 2 and 3, it can be elucidated that both the nucleation and grain growth behaviors are dependent on the incubation layer structure. The surface morphology, grain size, and incubation layer are strongly related to each other. As the thickness of the incubation layer increases, both the grain size and surface roughness decrease.

The effect of substrate temperature on the Raman spectra of the Si thin films is shown in Figure 4. It is well known that hydrogen dilution is an essential key factor in achieving μc-Si or poly-Si growth. Although a substrate temperature as high as 450 °C was used, the a-Si:H films could be formed using pure silane without any hydrogen dilution. Therefore, the samples shown here were deposited using a fixed hydro-

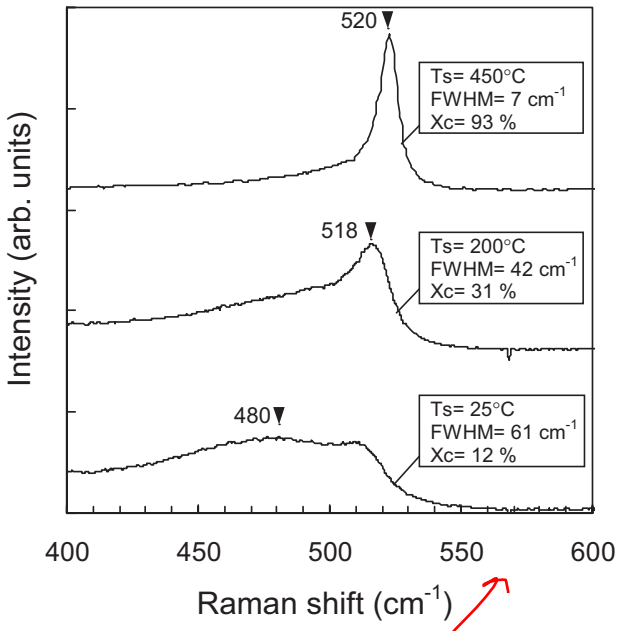

Fig. 4. A series of Raman spectra of silicon films deposited by HWCVD at various substrate temperatures, dependence of volume fraction of crystalline silicon X_c, and FWHM of silicon films as a function of substrate temperature.

gen dilution ratio ($H_2/SiH_4 = 10$) at various substrate temperatures. For $T_s < 150\,°C$, the Si film remains amorphous, while the film changes from a-Si:H to poly-Si when the substrate temperature increases above 150 °C. It is also found that the Raman peak shifts from 480 to 520 cm^{-1} when the substrate temperature increases from 25 to 450 °C. The corresponding FWHM narrows from 61 to 7 cm^{-1} and the X_c increases from 12 to 93 %. Similar results were also obtained by Han et al. in their HWCVD report.[26]

To further investigate the T_s effect on the Si film growth, the samples described in Figure 4 were examined by TEM. Typical TEM images of the high-T_s (450 °C) and low-T_s (25 °C) samples are shown in Figures 5 ($X_c = 93\,\%$) and 6 ($X_c = 12\,\%$), respectively. Heya et al. have reported that the poly-Si film can be deposited from the seed layer under high T_s conditions.[12] No incubation phase in the film was found for $T_s \geq 350\,°C$. In our case, the high-T_s (450 °C) sample shows clear grain boundaries as demonstrated by the plane view DF TEM image (Fig. 5a). Also illustrated in the inset of this figure is the corresponding diffraction pattern with (220) and (311) preferential orientations. These dominant diffraction rings suggest that the film appears singly crystallized at the initial stage and then grows epitaxially. As shown in the cross-section TEM image (Fig. 5b), a seed could be made at a high temperature of 450 °C. The V-shaped columns were grown from the glass surface. On the other hand, the Si film deposited at low substrate temperature presents a completely different growth mechanism. Figure 6a shows the plane view TEM image and its corresponding diffraction pattern of the low-T_s (25 °C) sample. No evident grain growth was observed in the cross-

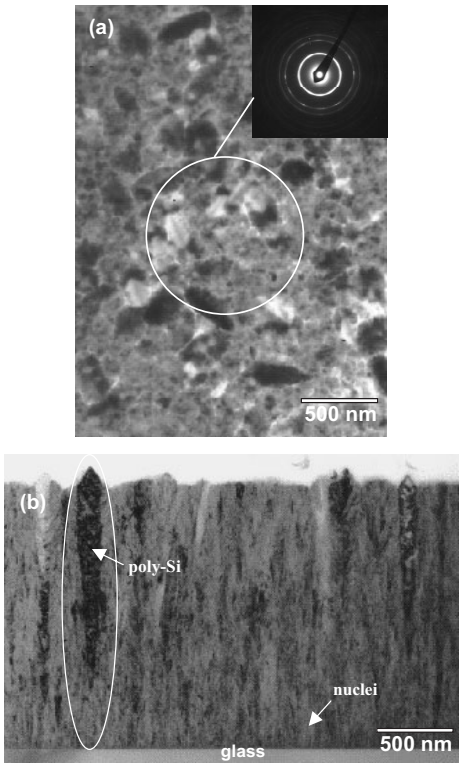

Fig. 5. TEM images of HWCVD poly-Si film; (a) dark field image and diffraction pattern, (b) cross-section image. The sample was fabricated under an SiH_4 flow rate of 5 sccm, a H_2 flow rate of 50 sccm, a filament temperature of 1700 °C, and a substrate temperature of 450 °C.

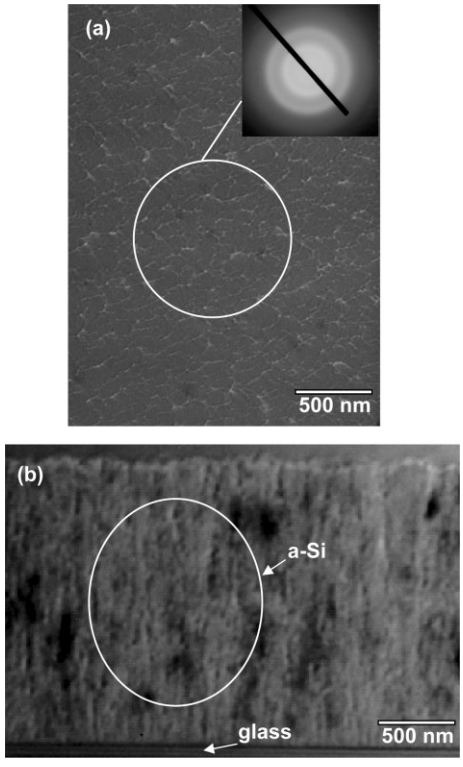

Fig. 6. TEM imags of HWCVD a-Si film; (a) dark field image and diffraction pattern, (b) cross-section image. The sample was fabricated under an SiH_4 flow rate of 5 sccm, a H_2 flow rate of 50 sccm, a filament temperature of 1700 °C, and a substrate temperature of 25 °C.

section TEM image (Fig. 6b). Because the grains are small, all of the reciprocal lattice points will be broadened by the shape effect. The diffraction patterns from an amorphous material (Fig. 6a) looks similar to that from a polycrystalline material (Fig. 5a), but the rings are broader and there is no speckle. The observed indistinct halo pattern indicates that the film is amorphous.

An approximate representation of the incubation and crystallization phase as functions of the H_2/SiH_4 ratio and substrate temperature are schematically shown in Figure 7. The Si films were grown under various H_2/SiH_4 ratios (on the left, $T_s = 350\,°C$) and substrate temperatures (on the right, $H_2/SiH_4 = 10$). The real and dotted lines identify the a-Si → (a + μc)-Si, and (a + μc)-Si → (μc + poly)-Si transi-

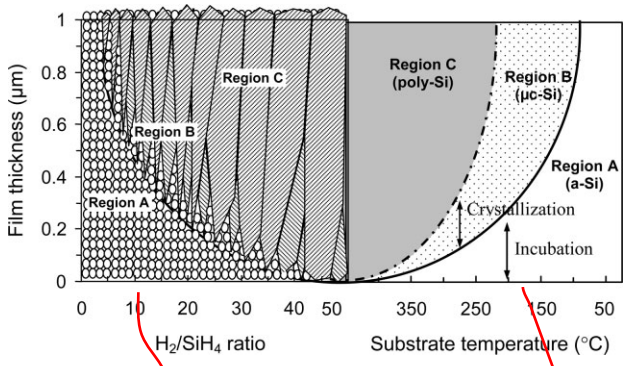

Fig. 7. Schematic representation of the a-Si, μc-Si, and poly-Si regions grown under various H_2/SiH_4 ratios and substrate temperatures. The substrate temperature was kept at 350 °C in the left part, and the H_2/SiH_4 ratio of 10 was used for the right part.

tions, respectively. The marked regions (B, C) represent crystallites and the white region shows the amorphous fraction. The incubation phase and crystallization phase are of great importance for the optoelectronic material properties. Region A shows that hydrogenated amorphous silicon films can be obtained by HWCVD using pure silane (SiH_4), low hydrogen dilution, and low growth temperature (<100 °C). At relatively higher hydrogen dilution, a μc-Si layer, consisting of small grains, is grown just above an a-Si incubation layer (region B). Microcrystalline silicon is a mixed phase material consisting of an a-Si, c-Si nano-crystallites and grain boundaries. During the film growth, crystallite formation starts with nucleation after an amorphous incubation phase. In the continuing layer deposition, clusters of crystallites grow (crystallization phase) until a saturated crystalline fraction is reached. By increasing the hydrogen dilution ratio and substrate temperature, this incubation layer becomes thin, and finally poly-Si is directly grown on the glass substrate (region C). It can be stated that these grains are enhanced by the presence of atomic hydrogen due to the chemical interaction with the growing surface.

3. Conclusion

A wide range of poly-Si films can be fabricated using the HWCVD method, showing the mature growth mechanism that this deposition process has attained. The initial HWCVD poly-Si growth stage and the relationships among the a-Si incubation layer were investigated. The hydrogen dilution ratio and growth temperature is a fingerprint of the amorphous to crystalline transition. The nuclei for grain growth were generated in the amorphous layer. Both the size and number of nuclei increased with the increase in the growth temperature. It is noteworthy that the growth mechanism was distinguished, which enabled us to control them independently by choosing the respective proper parameters. In this study, highly crystallized HWCVD poly-Si thin films ($X_c = 0.93$) and V-shaped columns structures without incubation layers were obtained.

4. Experimental

A HWCVD system with a load-lock chamber was used for this study. Tungsten wire (diameter: 0.5 mm; length: 240 mm) was used as the catalyzer, placed beneath the substrate at a distance of 48 mm. The catalyzer temperature was estimated using an electronic infrared thermometer placed outside a quartz window, and the electrical resistivity temperature dependence of the catalyzer. The substrate temperature was monitored using a thermocouple attached to the substrate holder. A shutter was placed right above the substrate during the adjustment of depositing parameters. Poly-Si films were deposited on glass (Corning 7059) substrates. In this study, the filament temperature ranged from 1500 to 1800 °C, and the substrate temperature ranged from 25 to 450 °C. The SiH_4 flow rate was kept at 5 sccm while the H_2 dilution gas was added up to 250 sccm. The reactant gases used in this work were SiH_4 diluted with H_2 (hydrogen dilution $\varphi = H_2/(H_2+SiH_4)$) and were carefully calibrated by mass flow controllers. The deposition pressure was keep at 10 Pa. Before the hot-wire deposition process, the chamber was pumped down to a base pressure of 2×10^{-5} Pa. Details of the deposition conditions are summarized in Table 1.

Table 1. Deposition conditions for poly-Si films.

Filament temperature (T_f)	1500–1800 °C
Substrate temperature (T_s)	25–450 °C
Catalyzer-substrate distance	48 mm
Surface area	754 mm^2
SiH_4 flow rate	5 sccm
H_2 flow rate	0–250 sccm
Gas pressure	10 Pa

The crystalline structure of the Si film was analyzed using Raman scattering spectroscopy (Nanofinder 30, Tokyo Instruments, Inc.) with a 632.8 nm laser source. The laser spot size was focused to about 1 μm diameter with a beam power of 2 mW. The measurements have been carried out first in calibration of the standard specimen (crystalline silicon wafer). The microstructures of poly-Si films were investigated by HRTEM (model: JEM-2010, JEOL) at 200 keV. The TEM specimens for the present study were prepared by mechanical thinning and ion milling. Two pieces of the samples were glued together face-to-face with Epoxy Bond 110 glue in order to obtain a cross-sectional preparation. During the TEM measurements, the objective lens was deliberately used in an under-focused deposition in order to highlight the void structure and grain boundary. The SIMS analysis has been performed by a CAMECA IMS-4f ion microscopy. A 5.5 keV Cs^+ primary

beam, focused to about 10 μm diameter, was scanned across an area of 200 × 200 μm^2. Typical beam currents were 10–30 nA.

Received: October 10, 2006
Revised: March 2, 2007

[1] A. H. Mahan, J. Carapella, B. P. Nelson, R. S. Crandall, I. Balberg, *J. Appl. Phys.* **1991**, *69*, 6728.
[2] H. Matsumura, *Jpn. J. Appl. Phys.* **1986,** *25*, L949.
[3] B. Nelson, E. Iwaniczko, A. H. Mahan, Q. Wang, Y. Xu, R. S. Crandall, H. M. Branz, *Thin Solid Films* **2001**, *395*, 292.
[4] A. Ledermann, U. Weber, C. Mukherjee, B. Schroeder, *Thin Solid Films* **2001**, *395*, 61.
[5] A. H. Mahan, *Solar Energy* **2004**, *77*, 931.
[6] A. Masuda, H. Matsumura, *Thin Solid Films* **2001**, *395*, 112.
[7] R. E. I. Schropp, *Thin Solid Films* **2002**, *403–404*, 17.
[8] S. Klein, F. Finger, R. Carius, O. Kluth, A. L. B. Neto, H. Wagner, M. Stutzmann, in *Proceedings of the 17th European Photovoltaic Solar Energy Conference* (Eds: B. McNelis, W. Palz, H. A. Ossenbrink, P. Helm), WIP, Munich **2001**, p. 2965.
[9] M. Otobe, S. Oda, *J. Non-Cryst. Solids* **1993**, *164/165*, 993.
[10] C. Godet, N. Layadi, P. Roca, Cabarrocas, *Appl. Phys. Lett.* **1995**, *66*, 3146.
[11] J. Zhou, K. Ikuta, T. Yasuda, T. Umeda, S. Yamasaki, K. Tanaka, *Appl. Phys. Lett.* **1997**, *71*, 1534.
[12] A. Heya, A. Izumi, A. Masuda, H. Matsumura, *Jpn. J. Appl. Phys., Part 1* **2000**, *39*, 3888.
[13] H. R. Moutinho, C. S. Jiang, J. Perkins, Y. Xu, B. P. Nelson, K. M. Jones, M. J. Romero, M. M. A. Jassim, *Thin Solid Films* **2003**, *430*, 135.
[14] M. Zhu, X. Guo, G. Chen, H. Han, M. He, K. Sun, *Thin Solid Films* **2000**, *360*, 205.
[15] H. Matsumura, H. Umemoto, A. Izumi, A. Masuda, *Thin Solid Films* **2003**, *430*, 7.
[16] J. K. Rath, F. D. Tichelaar, H. Meiling, R. I. E. Schropp, *Mater. Res. Soc. Symp. Proc.***1998**, *507*, 879.
[17] Z. Iqbal, S. Veprek, A. P. Webb, P. Capezzuto, *Solid State Commun.* **1981**, *37*, 993.
[18] T. Okada, T. Iwaki, K. Yamamoto, H. Kasahara, K. Abe, *Solid State Commun.* **1984**, *49*, 809.
[19] R. E. I. Schropp, *Thin Solid Films* **2001**, *395*, 17.
[20] J. K. Rath, A. J. Hardeman, C. H. M. Werf, P. A. T. T. Veenendaal, M. Y. S. Rusche, R. E. I. Schropp, *Thin Solid Films* **2003**, *430*, 67.
[21] H. R. Moutinho, C. S. Jiang, J. Perkins, Y. Xu, B. P. Nelson, K. M. Jones, M. J. Romero, M. M. A. Jassim, *Thin Solid Films* **2003**, *430*, 135.
[22] C. Manfredotti, F. Fizzotti, M. Boero, P. Polesello, E. Vittone, *Phys. Rev. B* **1994**, *50*, 24.
[23] I. Ferreira, E. Fortunato, R. Martins, *Thin Solid Films* **2003**, *427*, 231.
[24] S. Morrison, U. Das, A. Madan, *Solar Energy Mater. Solar Cells* **2003**, *76*, 281.
[25] S. Klein , T. Repmann, T. Brammer, *Solar Energy* **2004**, *77*, 893.
[26] D. Han, K. Wang, J. M. Owens, L. Gedvilas, B. Nelson, H. Habuchi, M. Tanaka, *J. Appl. Phys.* **2003**, *93*, 3776.

